Augmented Speed Control Scheme of Dual Induction Motors with Mutual Flux Angle Control Loop

DMYTRO KONDRATENKO*, ARKADIUSZ LEWICKI, KRZYSZTOF ŁUKSZA

Faculty of Electrical and Control Engineering
Gdańsk University of Technology
Narutowicza 11/12 str., 80-233 Gdańsk, Poland

e-mails: *dmytro.kondratenko@pg.edu.pl, arkadiusz.lewicki@pg.edu.pl,
krzysztof.luksza@pg.edu.pl

ORCID's
Dmytro Kondratenko – https://orcid.org/0000-0001-5322-8322
Arkadiusz Lewicki – https://orcid.org/0000-0003-2977-4192
Krzysztof Łuksza – https://orcid.org/0000-0003-0623-4329

Abstract: This paper proposes an augmented speed control scheme of dual induction motors fed by a five-leg voltage source inverter (VSI) with a common/shared-leg. An additional control loop is proposed here and based on the mutual flux angle- the difference between flux angular positions of the IMs. The main purpose of this research is to minimize the energy losses in the common inverter leg by controlling the mutual flux angle, at equal angular speeds of both motors. Simulation and experimental studies were carried out and the effectiveness of the proposed control method was proven. The PLECS software package was used for the simulation tests. The laboratory prototype was prepared for the experimental validation. All results were provided and discussed in this paper.

Key words: dual-motor drive, induction motors (IMs), five-leg voltage source inverter (FLVSI), rotor angle control, sensorless control.

1. Introduction

In recent decades, there has been an intensified research focus on multiphase drive systems. Most published articles describe five- or six-phase drive systems, [1 – 6]. A six-phase machine is a combination of two three-phase machines and is therefore more widely studied, [4 – 6]. Such a solution is proposed for various industry branches, including electric vehicles (EVs), railway traction and the concept of a more-electric aircraft. The five-phase system, which consists of a five-phase motor and a corresponding voltage inverter, offers several advantages over three-phase motors. These advantages include a potential 15% increase in torque using

third harmonic injection, higher fault tolerance, and the ability to operate with a damaged phase, [1 – 3]. Various analyzes were proposed to validate and prove these features, [7, 8]. Alongside multiphase systems, a number of multimotor drive systems have also been presented, [9 – 14]. Multimotor drive systems are used in many industrial applications, such as paper or textile industry, railway traction, and EVs, [9]. Two three-phase motors can be fed using a six-phase inverter, a five-phase inverter with a common leg, or a five-phase inverter with a common neutral point in the dc-link, [13,14].

Research in the field of dual-motor drive systems initially focused on developing appropriate modulation algorithms for five-phase VSIs, such as Sinusoidal and Space Vector PWMs, [9 – 11]. In [15], the authors note that it is possible to feed *n*-phase motors from a *(2n+1)*-phase inverter and propose a corresponding modulation algorithm. The next step was the development of a control system for such drives. Both modifications of the classic field-oriented control (FOC), direct torque control (DTC), and model predictive control (MPC) schemes were proposed for various combinations of motors, such as induction motors (IMs) and permanent magnet synchronous motors (PMSMs), [16 – 19]. Further research led to the development of new inverter topologies and corresponding modulation methods, [20, 21]. Despite the relative popularity of this topic, dual-drive systems continue to be actively researched, and in recent years, sophisticated control schemes and modulation techniques have been proposed, [22 – 24]. The most popular version of the dual-drive system consists of two IMs and a five-phase inverter with a common/shared leg. In recent years several control and modulation techniques were proposed, [19 – 22, 24], and the drive system's performance was discussed as well [25]. In this paper, one drive utilizes a conventional FOC scheme, while the second motor is controlled by a slightly modified FOC scheme. Moreover, an optimized SVPWM technique is used for both motors. In the SVPWM scheme used here, the initial stage of the modulation algorithm was modified, and the reference voltage vector position identification was removed from the algorithm. Comparison with the conventional SVPWM method shows that both approaches have similar performance in THD and dc-link voltage utilization. However, the optimized SVPWM technique offers a large improvement, up to 42%, in the processor usage time.

This article aims to explore the additional possibilities that a dual-drive system provides. By adjusting the mutual flux angle between the two IMs, it is possible to reduce energy losses by around 20% or achieve a higher modulation index than using conventional control methods. However, this feature is valid only in a limited operation range when both motors operate at the same speed. To achieve the set goals, the amplitude of the current in the common leg changes due to the mutual flux angle. The proposed control scheme differs from solutions described in the literature [19, 22, 24] by providing control over the mutual flux angle and minimizing the difference in angular speeds when the control signal is injected from an angle controller. Summarizing, the possible scenario of the proposed algorithm usage includes an analysis of the current operation conditions, to decide when the mutual angle control loop should be activated; depending on the control system objectives the extended modulation range or higher efficiency, by decreasing the total losses, can be achieved. For the operation points, when conditions do not fit within the limitations, the proposed mutual angle control loop will be inactive and the system behavior will be the same as in conventional solutions.

This paper is organized as follows: Section 2 describes the control algorithm, Sections 3 and 4 present the results of simulation and experimental studies, respectively, and Section 5 contains the conclusions.

2.   Proposed control scheme

The power circuit of the five-phase VSI is shown in Fig. 1. The common leg (phase "a" from Fig. 1.) is connected to the two IMs, and the independent control of two three-phase loads is possible. Conventional solutions, proposed for this dual-drive configuration, utilize the same control scheme for all operational conditions. Additional components in the control system can be used to increase the effectiveness of the drive system when both motors operate at the same speed. In [22], it was noticed that energy losses can be reduced by around 20%, by decreasing the amplitude of the common phase current. Nevertheless, the maximum modulation index for both motors is $M_1=M_2=0.577$. This paper proposes an improved control scheme, where losses can be reduced or the maximum modulation index can be increased up to $M_1=M_2=1.15$, depending on the needs for a specific application. Moreover, when the mutual flux angle control gets involved, the difference in angular speeds begins to rise, so the d-axis current correction unit minimizes this difference, as shown in this paper. The common leg current amplitude and the relation between the modulation index and the value of the mutual flux angle are shown in Fig. 2. (a) and (b), respectively.
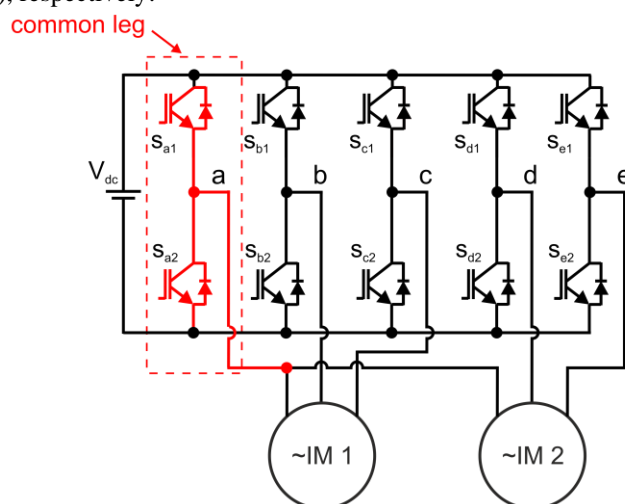

Fig. 1. Electrical connections of the five-leg VSI with a common leg and two three-phase motors.
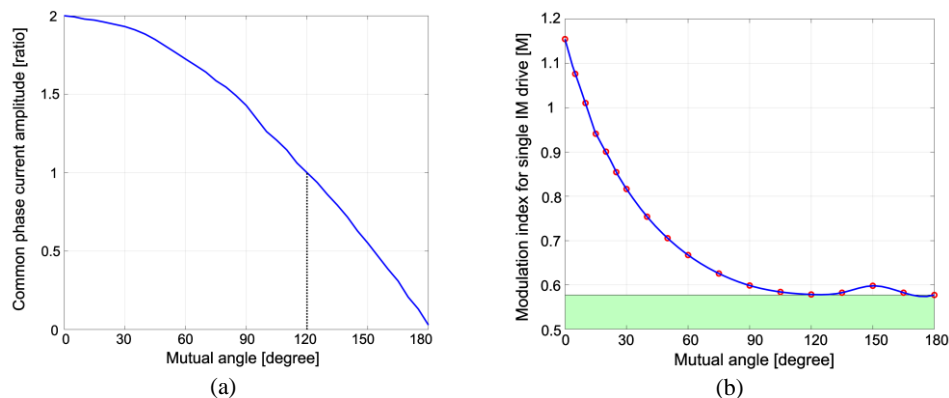
Fig. 2. The impact of the mutual angle on: the amplitude of the common leg current, shown as the ratio to the other phases (a); maximum modulation index for each motor M (b).

The proposed control scheme is based on the FOC scheme, so two FOC control systems were initially implemented. Sensorless control was also implemented for both, so two speed observer blocks were used in the control system. The FOC control scheme was modified for one of the motors, to inject an additional signal from the mutual angle controller. The mutual angle control and d-axis current correction unit were implemented as well. An optimized SVPWM technique was used here, as noted previously. The whole structure of the proposed control system is shown in Fig. 3.
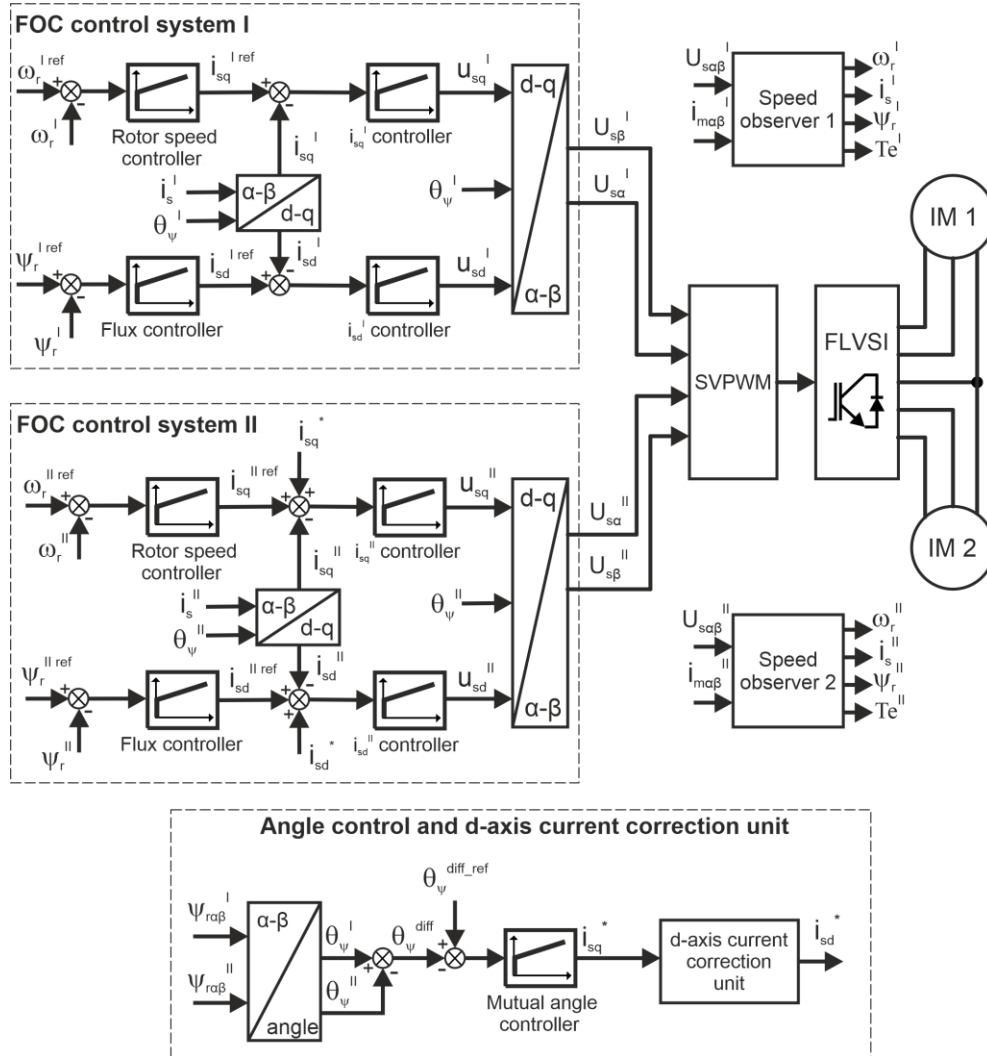
Fig. 3. The structure of the proposed control system.

The structure of the angle control block contains the angle calculation block, where the current value for each motor, $\theta_\psi^I, \theta_\psi^{II}$, is calculated, and the mutual angle PI controller. The controller output signal is added to the modified FOC scheme before q–axis current controller. At the same time, the d-axis current correction unit creates an additional control signal to minimize the rotor speed difference and keep the same dynamic for both motors. To obtain a proper d-axis current correction the control signal should be calculated based on the impact provided by the signal injection from the mutual angle controller. The mutual angle control structure interacts only with FOC control system II, so the FOC control system I remains unchanged. Moreover, the parameters of the FOC controllers are the same for both control schemes.

The induction motor model in $d - q$ coordinates, is given:

$$\frac{di_{sd}}{dt} = a_1 \cdot i_{sd} + a_2 \cdot \psi_{rd} + \omega_{\psi r} \cdot i_{sd} + a_4 \cdot u_{sd}, \tag{1}$$

$$\frac{di_{sq}}{dt} = a_1 \cdot i_{sq} - \omega_{\psi r} \cdot i_{sd} - \omega_r \cdot a_3 \cdot \psi_{rd} + a_4 \cdot u_{sq}, \tag{2}$$

$$\frac{d\psi_{rd}}{dt} = a_5 \cdot \psi_{rd} + a_6 \cdot i_{sd}, \tag{3}$$

$$\frac{d\psi_{rq}}{dt} = a_5 \cdot \psi_{rq} - (\omega_{\psi r} - \omega_r) \cdot \psi_{rd} + a_6 \cdot i_{sq}, \tag{4}$$

$$\frac{d\omega_r}{dt} = \frac{L_m}{L_r \cdot J} \cdot \psi_{rd} \cdot i_{sq} - \frac{1}{J \cdot m}, \tag{5}$$

where:

R_s, L_s are the stator resistance and inductance respectively,

R_r, L_r are the rotor resistance and inductance respectively,

L_m is the mutual inductance,

a_1- a_6 are the induction motor model coefficients, defined as follows:

$$a_1 = -\frac{R_s \cdot L_r^2 + R_r \cdot L_m^2}{L_r \cdot w_\sigma}, \ a_2 = \frac{R_r \cdot L_m}{L_r \cdot w_\sigma}, a_3 = \frac{L_m}{w_\sigma}, \ a_4 = \frac{L_r}{w_\sigma}, \ a_5 = -\frac{R_r}{L_r}, \ a_6 = R_r \cdot \frac{L_m}{L_r},$$

$$w_\sigma = \sigma \cdot L_r \cdot L_s = L_r \cdot L_s - L_m^2,$$

where: σ is the total leakage coefficient of the motor.

The rotor flux components in d-q coordinates for FOC scheme:

$$\begin{aligned} \psi_{rd} &= \psi_r, \\ \psi_{rq} &= 0; \end{aligned} \tag{6}$$

From (1) and (6) the relation between the d-axis current and the q-axis current, in steady state, can be obtained:

$$i_{sd} = -\frac{a_2 \cdot \psi_r + a_4 \cdot u_{sd}}{a_1 + \omega_{\psi r}}, \tag{7}$$

where: $\psi_r = -\frac{a_6 \cdot i_{sd}}{a_5} = L_m \cdot i_{sd}$, and $\omega_{\psi r} = \frac{R_r \cdot L_m \cdot i_{sq}}{L_r \cdot \psi_r} + \omega_r$.

Considering these dependencies, the final equation takes the form of:

$$i_{sd} = -\frac{L_r \cdot u_{sd} + R_r \cdot i_{sq} \cdot (L_r \cdot L_s - L_m^{\ 2})}{-R_s \cdot L_s^{\ 2} + \omega_r \cdot L_r^{\ 2} \cdot (L_r \cdot L_s - L_m^{\ 2})} , \tag{8}$$

The q-axis current impact on the d-axis current is small, due to the motor parameters and eq. (8). So a proportional controller should be added before an additional signal injection to the d-axis current control loop. Utilizing the output signal from the mutual angle controller as the q-axis current in (8) and with proportional controller implementation the additional signal injection to the d-axis current can be calculated as follows:

$$i_{sd}^* = k_p \cdot \left(-\frac{L_r \cdot u_{sd} + R_r \cdot i_{sq}^* \cdot (L_r \cdot L_s - L_m^{\ 2})}{-R_s \cdot L_s^{\ 2} + \omega_r \cdot L_r^{\ 2} \cdot (L_r \cdot L_s - L_m^{\ 2})} \right). \tag{9}$$

where: k_p is the gain of the P controller, and i_{sq}^* is the output signal from the mutual flux angle controller.

3.   Simulation results

The PLECS software package was used for simulation studies. During these studies, the main focus was set on the drive system behavior investigation. Initially, the idea of decreasing the common leg current amplitude was verified, and then several working points were tested to prove the reliability of the curve presented in Fig. 2. Next, the ability to utilize higher modulation indexes was verified. Finally, the loss analysis was provided and the possibility of total energy loss reduction was shown.
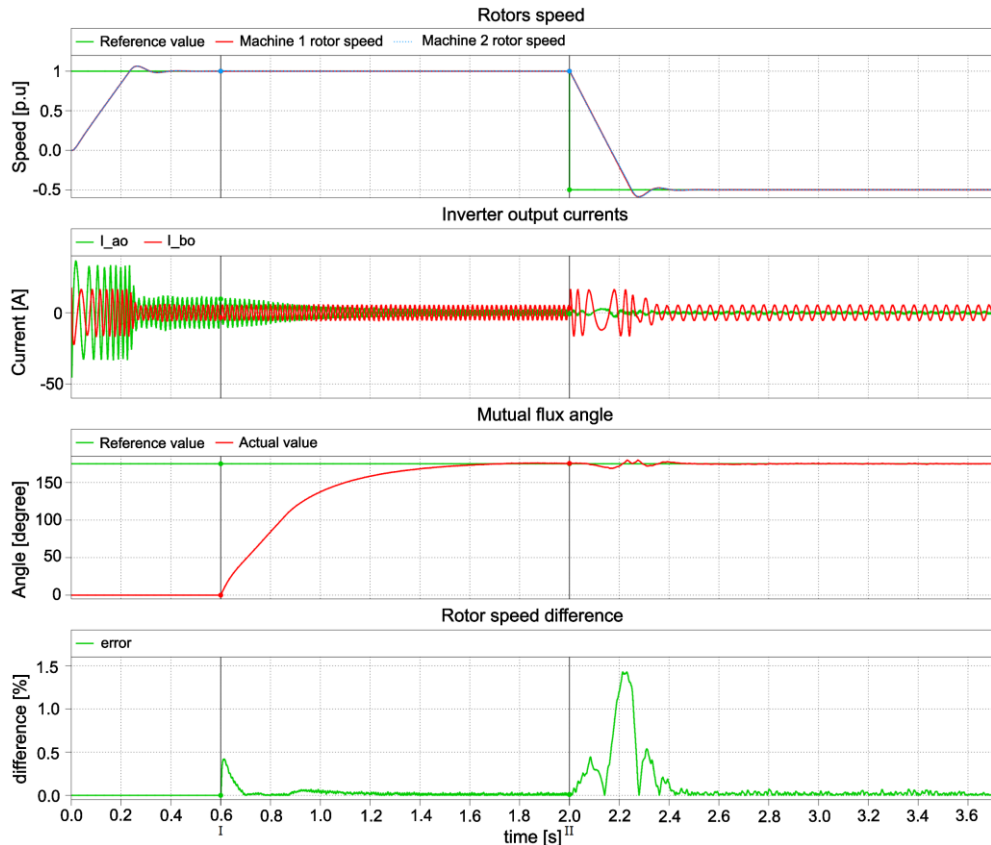
Fig. 4. Machines' rotor speeds, inverter currents (common leg and in one of the other phases), the mutual flux angle and the rotor speed difference under a step change in the mutual flux angle (from 0 to 175), and under a step change in rotor speed, from 1 to -0.5 (the angle is 175 degrees).

Figure 4 shows the system response to a step change in the mutual flux angle, from 0 to 180 degrees, at the moment of 0.6 s. The system response to a step change in the rotor speed, from 1 to -0.5, is shown as well. System behavior in the dynamic and stable state modes is presented. Various mutual flux angle values were investigated and the results shown in Fig. 5. The mutual flux angle value was changed from 0 to 30, then to 120, 150, and finally to 180 degrees. As might be noticed the current amplitude in the common phase decreases, so the losses are reduced simultaneously. The rotor speeds, inverter output currents, the value of the mutual flux angle, and rotor speed difference are shown in Fig. 4 and Fig. 5. As shown in the obtained results, the rotor speed difference does not exceed 0.5% in stable-mode and 2% in dynamic-mode operation.
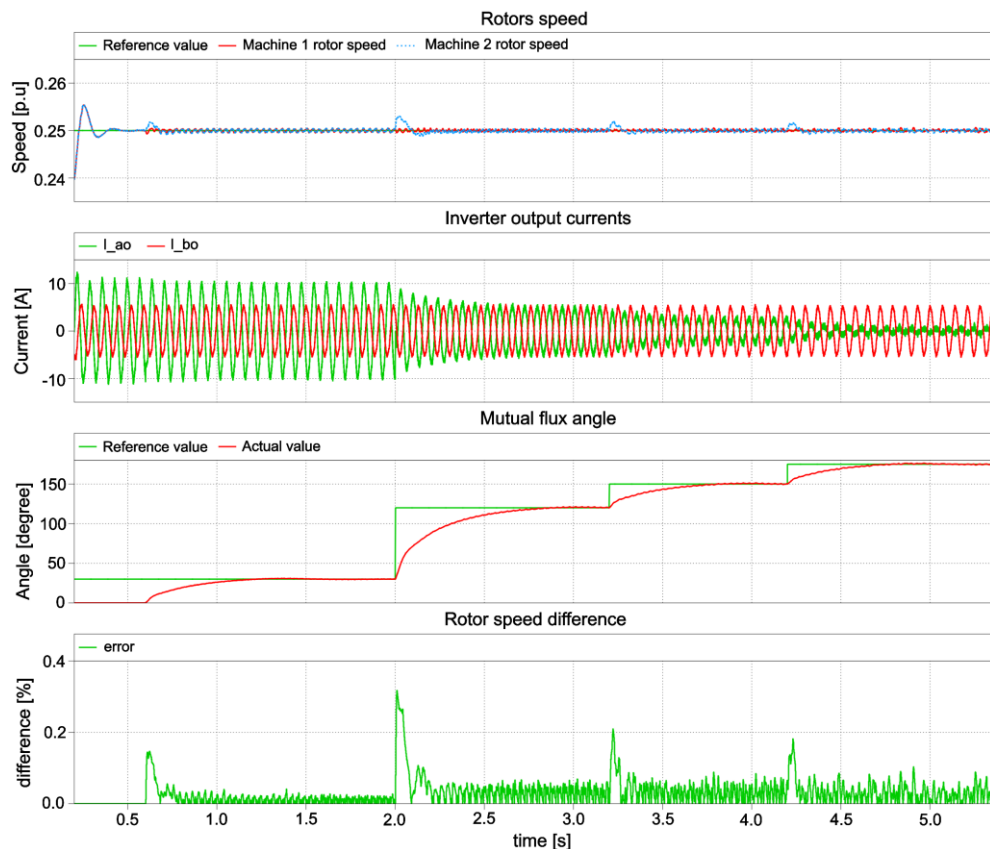
Fig. 5. Machines' rotor speeds, inverter currents (common leg and in one of the other phases), the mutual flux angle and the rotors' speed difference under a step change in mutual flux angle (from 0 to 30, then to 120, to 150 and to 175 degrees).

Figure 6 shows the dynamic system response to a step change in the rotor speed, from 1 to 2 and then to 1.5. The rotor speeds, inverter output currents, the mutual flux angle, and the minimal zero time are shown. The minimal zero time shows the current time reserve before the SVPWM algorithm will cross into the overmodulation zone. The closer the zero time is to the value of 0 the smaller time reserve is available. In Fig. 6 the system works in the overmodulation zone (the duration of zero vector is equal or close to zero) during the speed change from 1 to 2, at the time interval of 1.177 – 1.251 *s*. However, when the rotor speeds are set to 2, the modulation indexes in the stable-state mode are $M_1=M_2=1$.

Figure 7 shows the dynamic system response to a step change in the mutual angle, from 0 to 175 degrees and then to 5 degrees. The currents of machines 1 and 2 are given, and the shape of these currents' waveforms is symmetrical. The machines' rotor speeds and inverter output currents are shown as well. During a change in the value of the mutual flux angle, the common phase current was significantly reduced (when the angle value was 175 degrees). It causes

asymmetry in the inverter output currents, however, this asymmetry has no impact on the machines' currents.
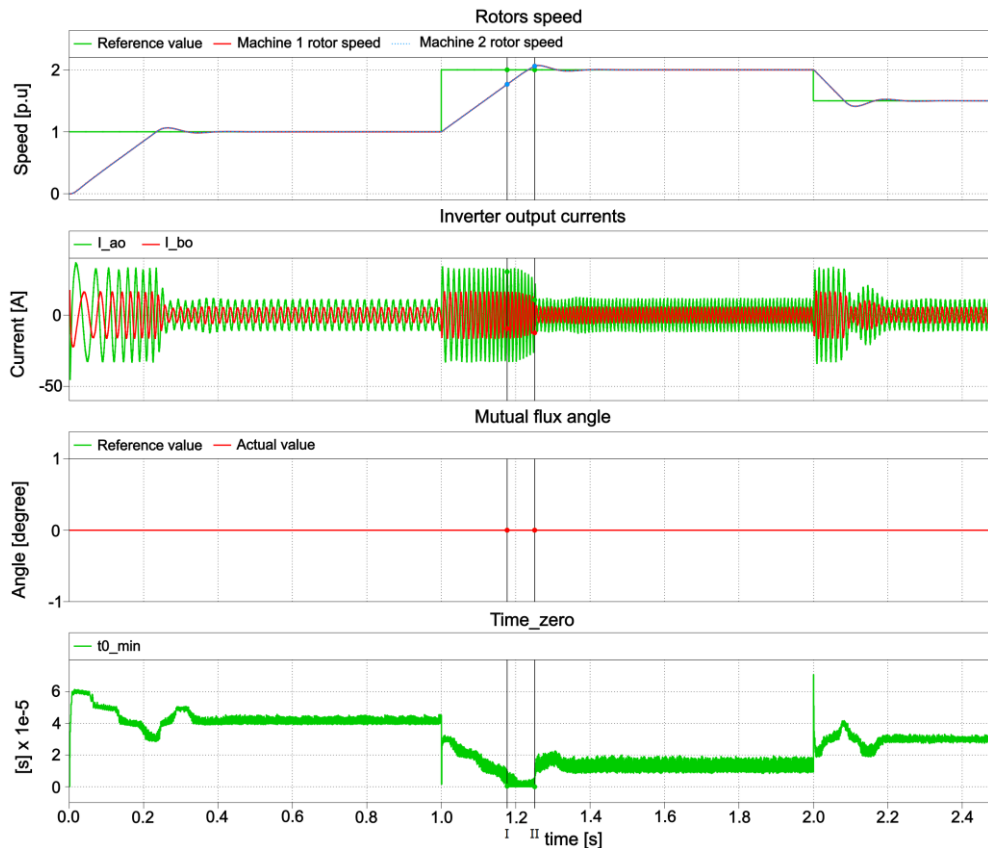

Fig. 6. Machines' rotor speeds, inverter currents (common leg and in one of the other phases), the mutual flux angle and the zero vector duration (Time_zero) under a step change in the rotor speed, from 1 to 2 and then to 1.5 (angle is 0 degree).

The total energy losses are given in Fig. 8., where the total losses for all the inverter legs are given. Inverter total energy loss is shown, while the mutual angle was changed from 0 to 120 and then to 175 degrees. To estimate the conductional and switching losses, the transistor model was taken from the list provided by PLECS software. These models were created using the datasheet parameters, provided by the manufacturer. The mutual angle of 175 degrees was chosen as the optimal working point. For this value, the estimated total energy loss is *18 W*, for 120 degrees the estimated total energy loss is *22 W*, and for a mutual angle of 0 degrees the total energy loss increases to *26.7 W*. In conventional solutions, the common leg current remains uncontrolled, and the mutual angle can take any value during the working cycle. In [22] the behavior of such systems is shown, where the amplitude of the common leg current can be two times higher than the current in other phases. The proposed solution allows to reduce the amplitude of the current in the common phase, as shown in Fig. 4 and 7.

To compare the proposed solution with the conventional control scheme three operation points were analyzed. In the analyzed points the mutual angle takes values of 0, 120 and 175 degrees under conventional control. With those angles the sum of energy losses in all inverter phases are *26.7 W*, *22 W*, and *18 W* for the conventional scheme. The proposed method allows to control the common phase current and thus allows to reduce the common phase losses. The sum of losses with the proposed control is *18 W* (the mutual angle is 175 degrees). Considering this data, the total loss can be reduced by *8.7 W*, *4.7 W*, and *0 W*, at each of these operation points. Selected operation points show a loss reduction of 32.5%, 17.6% and 0% respectively. For 90 degrees the total loss can be reduced by *6.1 W* or 22%.
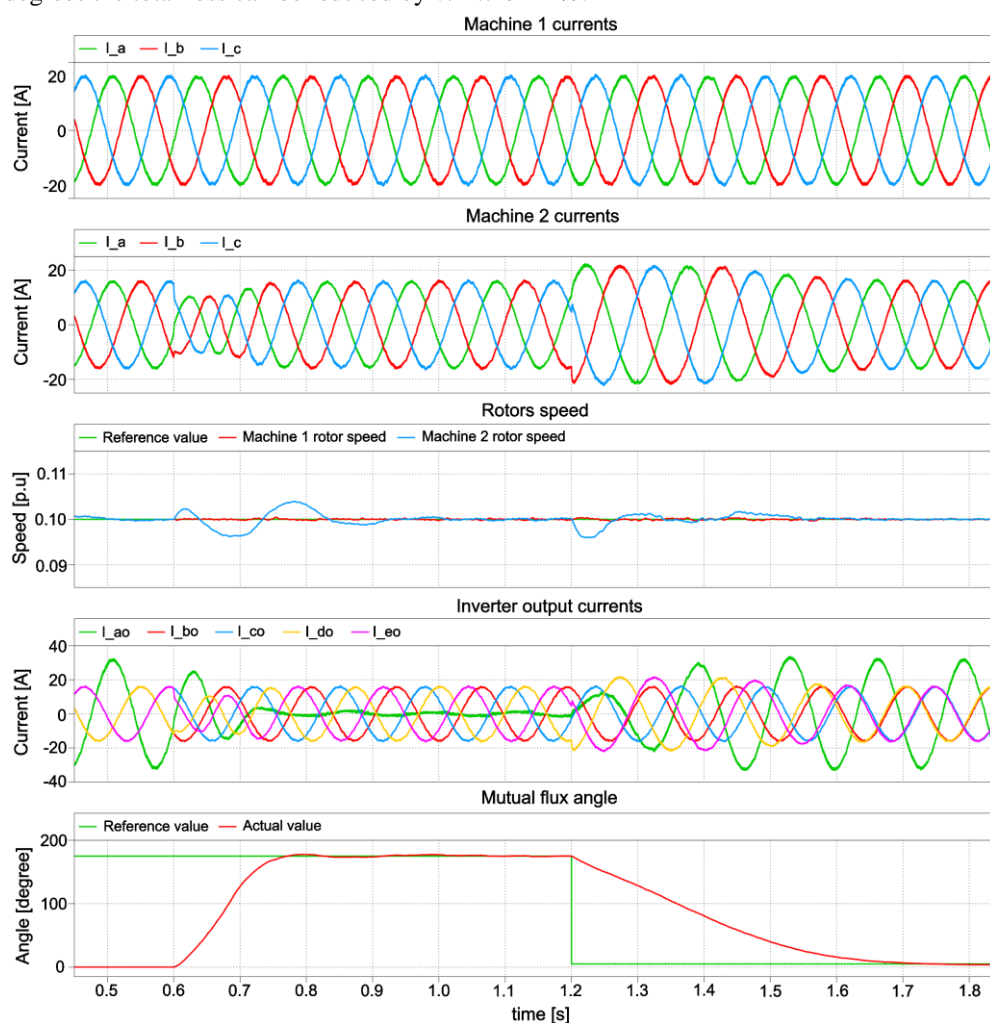
Fig. 7. Machines currents, inverter output currents, the mutual flux angle and the machines rotor speeds under a step change in mutual angle, from 0 to 175 degrees and then to 5 degrees.
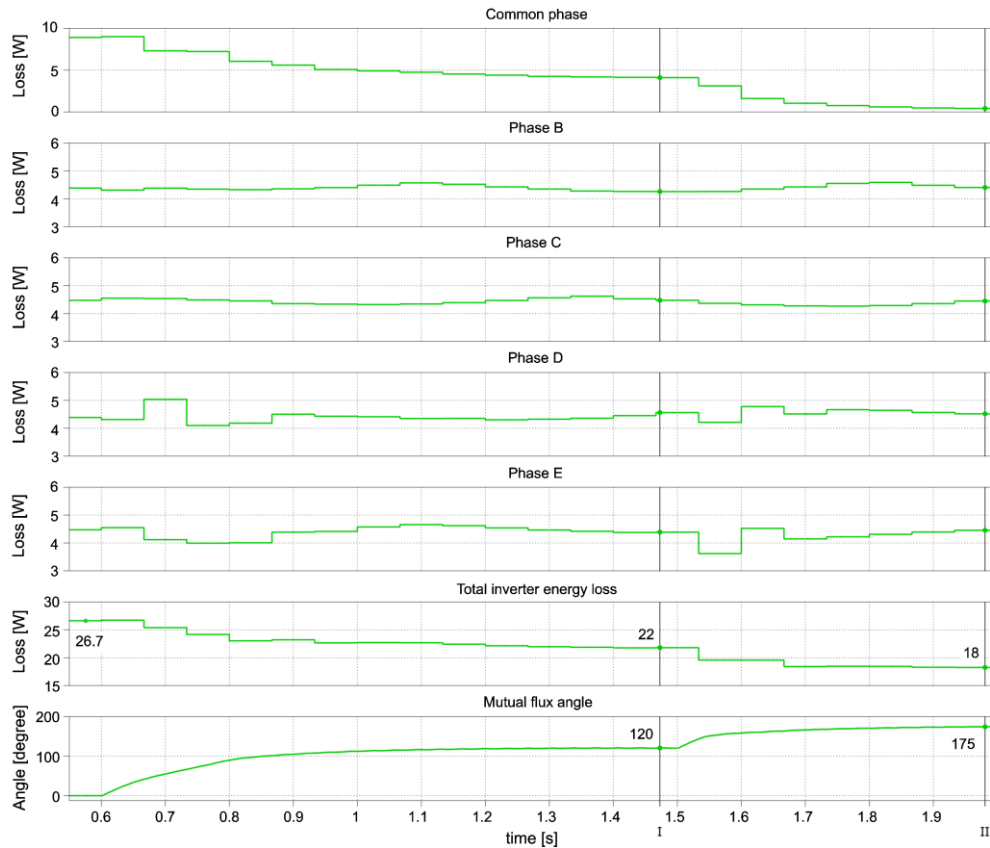
Fig. 8. Total energy loss at each phase individually, the total inverter losses and the mutual flux angle under a step change in the mutual angle, from 0 to 120 and then to 175 degrees.

4. Experimental results

The experimental studies were carried out using a five-leg VSI connected to a set of dual induction motor drives, as shown in Fig. 9. The experimental research consisted of the analysis of the system response in dynamic- and stable-states during the changes in the mutual flux angle and the angular speed of both motors. Figure 9 (a) describes the system response to the mutual flux angle change, when the mutual flux angle values were step-changed from 0 to 60 and then to 120 degrees. The amplitude of the common-leg current (i_{ma} from Fig. 10) is decreasing during changes in the value of the mutual flux angle, as expected. The small changes in the angular speed might be noticed, however, the speed difference between both motors does not exceed 1%. Figure 10 (b) shows the changes in system behavior under the mutual flux angle change from 120 to 150 and then to 175 degrees. The estimated rotor speeds, currents of the common-leg and one other phase, and the mutual flux angle values are shown in Fig. 10. The values of the mutual angle controller gains, K_p and K_i, are equal to 0.3 and 0.001, respectively.
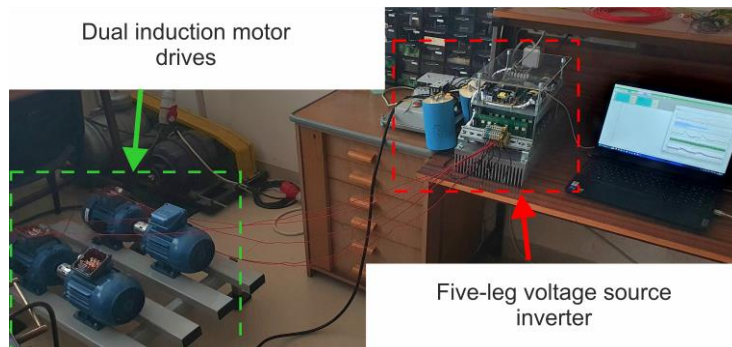
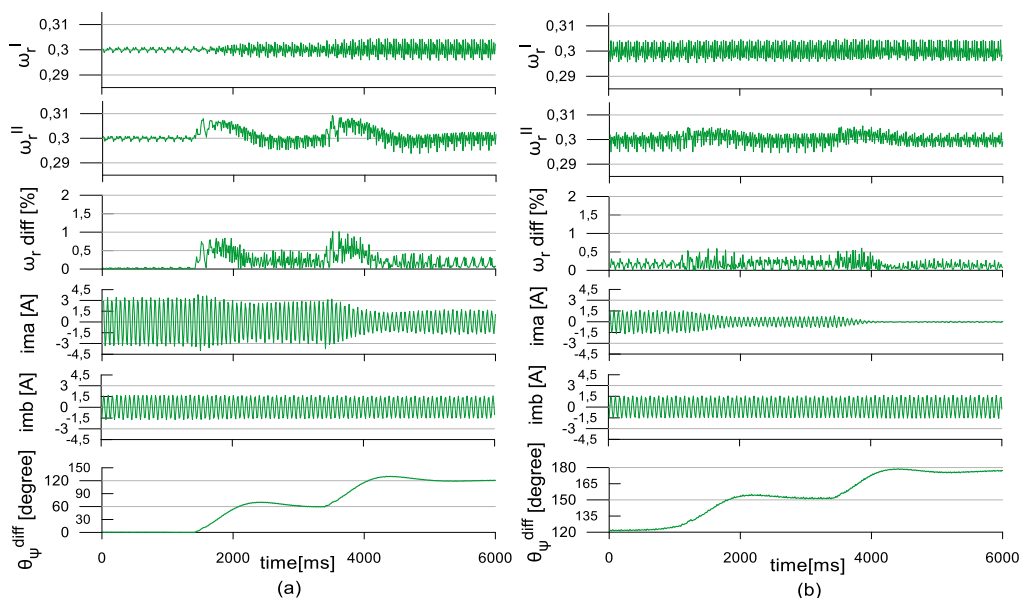Fig. 9. The experimental setup: dual-motor drive system and five-leg VSI.

Fig. 10. Rotor speeds, the rotors' speed difference, inverter currents (common leg and in one of the other phases), the estimated mutual flux angle under a step change in the mutual flux angle, from 0 to 60 and then to 120 degrees (a), and from 120 to 150 and then to 175 degrees (b)

Figure 11 shows the system response to step changes in the mutual flux angle, as in Fig. 10, however, the changes in the estimated flux value were also indicated. The dynamic system response to a speed change is shown in Fig. 12. Figure 12 (a) shows the speed values of both motors, the current of the common-leg, the flux component value, and the mutual flux angle under the increase in the angular speed. Figure 12 (b) represents the system behavior during the speed decrease. In the dynamic-state, the mutual flux angle controller tries to keep the value near the reference value. However, the nature of the proposed control scheme limits the regulation possibilities, to keep the dynamic characteristics. Due to this, the steady-state mode is preferable. During the speed change, the error in the mutual flux angle does not exceed 23.5%.
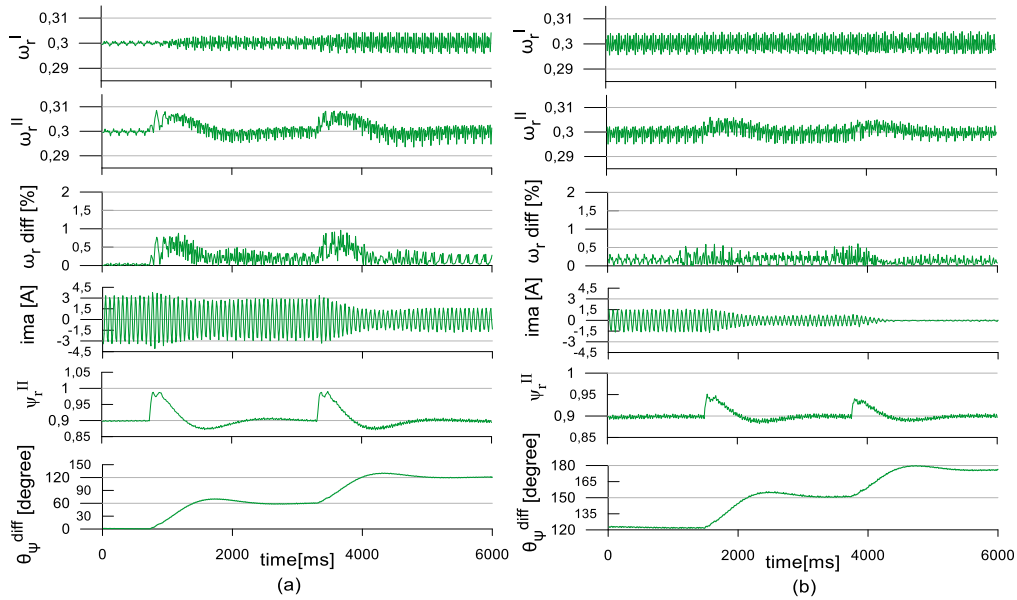
Fig. 11.   Rotor speeds, the rotors' speed difference, inverter common phase current, the estimated flux component and the mutual flux angle values under a step change in the mutual flux angle: from 0 to 60 and then to 120 degrees (a), and from 120 to 150 and then to 175 degrees (b)
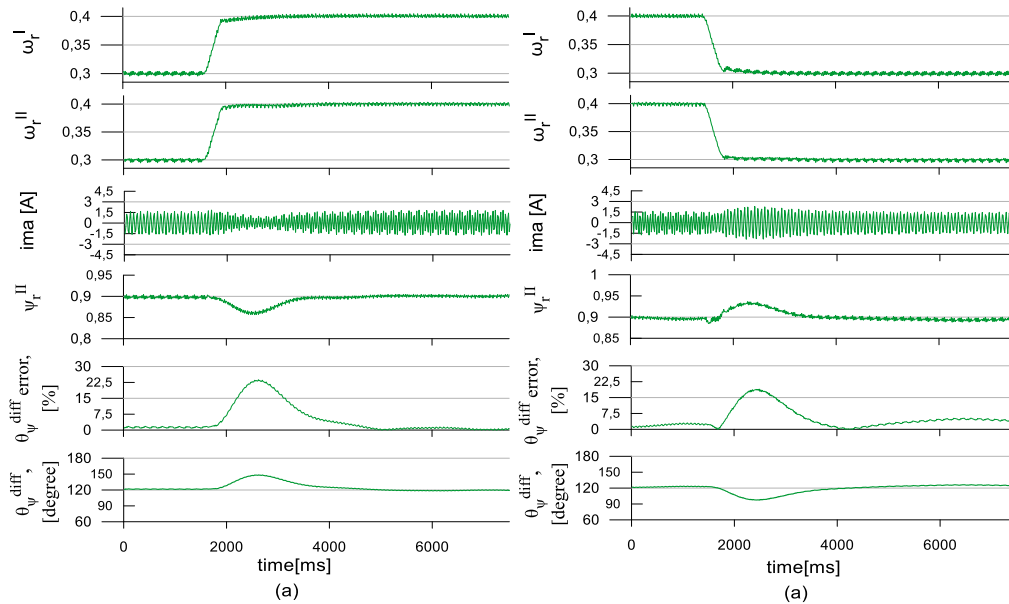

Fig. 12. Rotor speeds, inverter common phase current, the estimated flux component, the mutual flux angle error, and the mutual flux angle values under a step change in angular speed: from 0.3 to 0.4 (a), and from 0.4 to 0.3 (b)
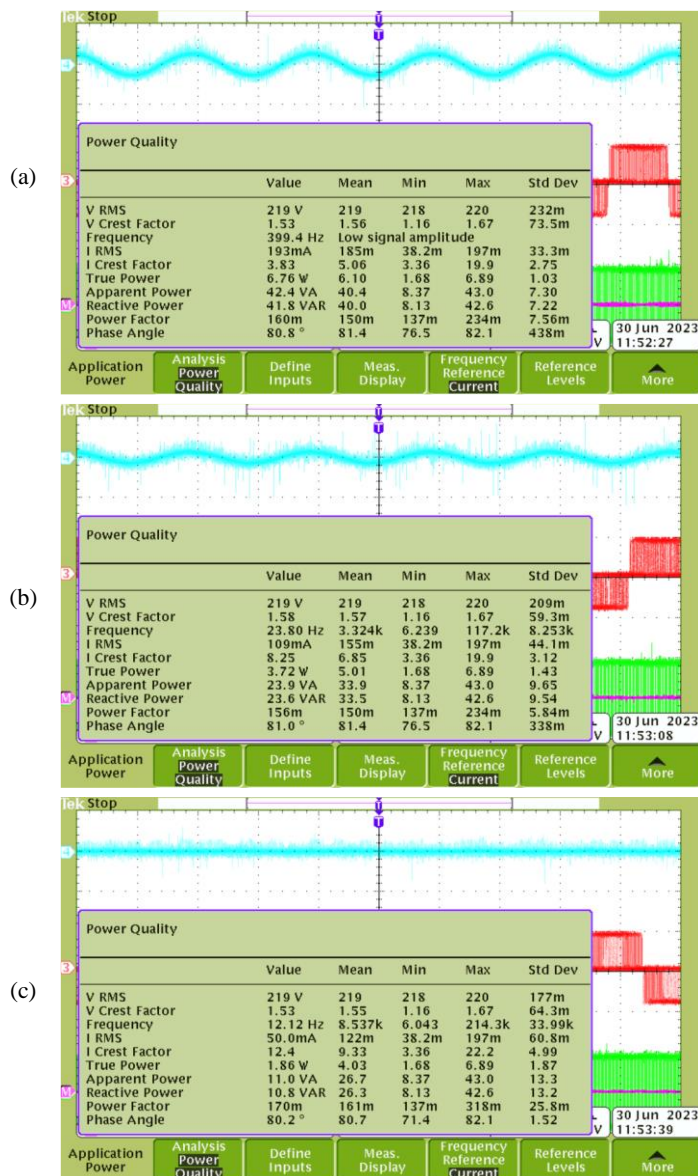
Fig. 13.   Common leg power quality analysis, the mutual flux angle is 0 (a) 120 (b) and 175 (c) degrees.

The power quality analysis was carried out to verify the possibility of loss reduction under the proposed control scheme. The Tektronix oscilloscope with power analyzer module was used for analysis purposes. Figure 13 shows the true power values in the common leg for different mutual angle values of 0, 120 and 175 degrees. The true power in the common phase is 6.76W, 3.72W and 1.86W for 0, 120 and 175 degrees, respectively. Therefore, the true power in the common

phase can be reduced by 72.5%, 45.0% and 0%, in comparison with the conventional control schemes. Simultaneously with the true power reduction, the conduction losses are reduced, confirming the correctness of the proposed control method. According to these results, we can estimate the total inverter power as 21.64W, 18.6W, and 16.74W for 0, 120 and 175 degrees, respectively. The corresponding total inverter power reduction is 22.7% for 175 degrees, 14% for 120 degrees, and 0% for 0 degrees.

5. Conclusions

The proposed control scheme proves the effectiveness of the idea of the mutual flux angle control while showing several limitations of this approach. Provided studies present the possibility of a decrease in energy losses by around 20% when the mutual flux angle value is set to 180 degrees. The error in the angular speed was sufficiently reduced by the d-axis current correction unit. However, some limitations of this method should be mentioned as well. The mutual flux angle control loop should be used in stable-state mode when the angular speeds of both motors are the same. The second limitation is each motor's electromagnetic torque, as due to the nature of the mutual flux angle, for loss reduction the torques should be equal, as well. Summing up, the presented mutual flux angle control scheme should be considered as an additional part of the existing systems and should be used for a limited operation range. According to the possibilities and limitations of the proposed control scheme, the full spectrum of the industrial applications where dual-motor drive systems are used (EVs, railway traction, paper and textile industries, etc.) should be considered as a possible sphere of usage. Even if the operation conditions fit the requirements from time to time, when dual-motor drives operate with the same speed and torque, the proposed control scheme allows to achieve a higher system efficiency. Summarizing, the proposed control scheme would be able to control drives effectively and decrease the energy losses, during the life cycle of the drive system.

References

[1] Levi E., Bojoi R., Profumo F., Toliyat H.A., Williamson S., *Multiphase induction motor drives - a technology status review,* Electric Power Applications IET, vol. 1, no. 4, pp. 489–516 (2007), DOI: 10.1049/iet-epa:20060342.

[2] Cao W., Mecrow B.C., Atkinson G.J., Bennett J.W., Atkinson D.J., *Overview of Electric Motor Technologies Used for More Electric Aircraft (MEA),* IEEE Transactions on Industrial Electronics, vol. 59, no. 9, pp. 3523–3531 (2012), DOI: 10.1109/TIE.2011.2165453.

[3] Barrero F., Duran M.J., *Recent Advances in the Design, Modeling, and Control of Multiphase Machines—Part I,* IEEE Transactions on Industrial Electronics, vol. 63, no. 1, pp. 449–458 (2016), DOI: 10.1109/TIE.2015.2447733.

[4] Che H.S., Levi E., Jones M., Hew W.P., Rahim N.A., *Current Control Methods for an Asymmetrical Six-Phase Induction Motor Drive,* IEEE Transactions on Power Electronics, vol. 29, no. 1, pp. 407–417 (2014), DOI: 10.1109/TPEL.2013.2248170.

[5] Hu Y., Zhu Z.Q., Odavic M., *Comparison of Two-Individual Current Control and Vector Space Decomposition Control for Dual Three-Phase PMSM,* IEEE Transactions on Industry Applications, vol. 53, no. 5, pp. 4483–4492 (2017), DOI: 10.1109/TIA.2017.2703682.

[6] Chen H., Gao Q., Yang T., Summer M., *Fundamental PWM Excitation Based Rotor Position Estimation for a Dual Three-Phase Permanent Magnet Synchronous Machine,* in IEEE Journal of Emerging and Selected Topics in Industrial Electronics, vol. 4, no. 2, pp. 659–668 (2023), DOI: 10.1109/JESTIE.2022.3223880.

[7] Listwan J.J., *Analysis of fault states in drive systems with multi-phase induction motors,* Archives of Electrical Engineering, vol. 68, no. 4, pp. 817–830 (2019), DOI: 10.24425/aee.2019.130685.

[8] Tani A., Mengoni M., Zarri L., Serra G., Casadei D., *Control of Multiphase Induction Motors With an Odd Number of Phases Under Open-Circuit Phase Faults,* IEEE Transactions on Power Electronics, vol. 27, no. 2, pp. 565–577 (2012), DOI: 10.1109/TPEL.2011.2140334.

[9] Jones, M., Levi, E., Wright, P., Vukosavic, S. N., Dujic, D., *Five-leg inverter PWM technique for reduced switch count two-motor constant power applications,* IET Electric Power Applications, vol. 2, no. 5, pp. 275–287 (2008), DOI: 10.1049/iet-epa:20070497.

[10] Lee J.H., Lee J.S., Ryu J.H., *Carrier-Based Discontinuous PWM Method for Five-Leg Inverter,* IEEE Access, vol. 8, pp. 100323–100336 (2020), DOI: 10.1109/ACCESS.2020.2998177.

[11] Geng Q. et al., *An Improved PWM Method of Five-Leg VSI Fed Dual-PMSM System With Duty Cycles Regulation,* IEEE/ASME Transactions on Mechatronics, vol. 27, no. 6, pp. 5771–5779 (2022), DOI: 10.1109/TMECH.2022.3190690.

[12] Lim C.S., Levi E., Jones M., Rahim N. A., Hew W.P., *A Comparative Study of Synchronous Current Control Schemes Based on FCS-MPC and PI-PWM for a Two-Motor Three-Phase Drive,* IEEE Transactions on Industrial Electronics, vol. 61, no. 8, pp. 3867–3878 (2014), DOI: 10.1109/TIE.2013.2286573.

[13] Jing G., Zhou C., *Control Strategy for a Five-Leg Inverter Supplying Dual Three-Phase PMSM,* IEEE Access, vol. 8, pp. 174480–174488 (2020), DOI: 10.1109/ACCESS.2020.3025392.

[14] Jacobina C.B., dos Santos E.C., da Silva E.R.C., Correa M.B.d.R., Lima A.M.N., Oliveira T.M., *Reduced Switch Count Multiple Three-Phase AC Machine Drive Systems,* IEEE Transactions on Power Electronics, vol. 23, no. 2, pp. 966–976 (2008), DOI: 10.1109/TPEL.2007.915027.

[15] Dujic D., Jones M., Vukosavic S.N., Levi E., *A General PWM Method for a (2n + 1) -Leg Inverter Supplying n Three-Phase Machines,* IEEE Transactions on Industrial Electronics, vol. 56, no. 10, pp. 4107–4118 (2009), DOI: 10.1109/TIE.2009.2014909.

[16] Xu F., Shi L., Li Y., *The Weighted Vector Control of Speed-Irrelevant Dual Induction Motors Fed by the Single Inverter,* IEEE Transactions on Power Electronics, vol. 28, no. 12, pp. 5665–5672 (2013), DOI: 10.1109/TPEL.2013.2259263.

[17] Lim C.S., Rahim N.A., Hew W.P., Levi E., *Model Predictive Control of a Two-Motor Drive With Five-Leg-Inverter Supply,* IEEE Transactions on Industrial Electronics, vol. 60, no. 1, pp. 54–65 (2013), DOI: 10.1109/TIE.2012.2186770.

[18] Wang W., Zhang J., Cheng M., Cao R., *Direct Torque Control of Five-leg Dual-PMSM Drive Systems for Fault-tolerant Purposes,* Journal of Power Electronics, vol. 17, no. 1, pp. 161–171 (2017), DOI: 10.6113/jpe.2017.17.1.161.

[19] Hasoun M., El afia A., Khafallah M., *Field Oriented Control of Dual Three-Phase PMSM Based Vector Space Decomposition for Electric Ship Propulsion*, Proceedings of 2019 International Conference of Computer Science and Renewable Energies (ICCSRE), Agadir, Morocco, pp. 1–6 (2019), DOI: 10.1109/ICCSRE.2019.8807703.

[20] Nguyen T.D., Lee H.H., *Dual Three-Phase Indirect Matrix Converter With Carrier-Based PWM Method,* IEEE Transactions on Power Electronics, vol. 29, no. 2, pp. 569–581 (2013), DOI: 10.1109/TPEL.2013.2255067.

[21] Odeh C.I., Lewicki A., Morawiec M., Ojo J.O., *A Five-Leg Three-Level Dual-Output Inverter,* IEEE Transactions on Circuits and Systems II: Express Briefs, vol. 70, no. 2, pp. 690–694 (2023), DOI: 10.1109/TCSII.2022.3211273.

[22] Lim Y.S., Lee J.S., Lee K.B., *Advanced Speed Control for a Five-Leg Inverter Driving a Dual-Induction Motor System,* IEEE Transactions on Industrial Electronics, vol. 66, no. 1, pp. 707–716 (2019), DOI: 10.1109/TIE.2018.2831172.

[23] Chaoui H., Khayamy M., Okoye O., Gualous H., *Simplified Speed Control of Permanent Magnet Synchronous Motors Using Genetic Algorithms,* IEEE Transactions on Power Electronics, vol. 34, no. 4, pp. 3563–3574 (2019), DOI: 10.1109/TPEL.2018.2851923.

[24] Choi D., Lee J.S., Lim Y.S., Lee K.B., *Priority-Based Model Predictive Control Method for Driving Dual Induction Motors Fed by Five-Leg Inverter,* IEEE Transactions on Power Electronics, vol. 38, no. 1, pp. 887–900 (2023), DOI: 10.1109/TPEL.2022.3203961.

[25] Farhi S.E., Sakri D., Golèa N., *High-performance induction motor drive based on adaptive super-twisting sliding mode control approach,* Archives of Electrical Engineering, vol. 71, no. 1, pp. 245–263 (2023), DOI: 10.24425/aee.2022.140208.